

Finite-Set Model Predictive Direct Power Control of Grid Connected Current Source Inverter

Hamza Feroura¹, Fateh Krim¹, Billel Talbi¹, Abdelbaset Laib¹, Abdesslam Belaout¹

¹*Department of Electronics Engineering, Setif 1 University,
Setif, 19000, Algeria
h_feroura@univ-setif.dz*

Abstract—This paper proposes a novel control strategy for grid connected current source inverter (CSI) without using a phase locked loop (PLL). The proposed finite set model predictive direct power control (FS-MPDPC) is based on direct power control (DPC) and model predictive control (MPC), and it is introduced for the first time for CSIs. The FS-MPDPC controls separately the active and reactive power, using an appropriate discrete-time prediction model to predict the future behaviour of the powers to be injected into the grid, and a cost function for the selection of the optimal control signals to be applied on the switches of the power converter. The proposed control technique is simulated in Matlab/simulink® software. The obtained results verify the effectiveness of this method during different test.

Index Terms—Current source inverter; direct power control; model predictive control; sliding mode observer.

I. INTRODUCTION

Renewable energy resources are environmentally clean, free, and abundant in the nature. These power sources are heavily dependent on power electronics for conversion and control [1].

Usually Voltage source inverters (VSIs) are used to interface DC sources with utility grid. However, recently, CSIs are seen as matter of great importance, due the features they offer, such like reliability, ruggedness, inherent short circuit protection, low harmonic distortion. But the primary advantage of CSIs as compared to VSIs is that CSIs are capable to transfer power from a low DC voltage to a higher AC voltage level in single stage with no need for a cascaded boost converter of a step up transformer. Thus, AC voltages required in certain applications can be obtained from a low voltage source. Also this makes CSI suitable to interface renewable distributed generation (DG) sources or DC microgrids with AC grids for power injection [1].

Recently a new control strategy has appeared in the field of control of power converters, named finite-set model predictive control (FS-MPC). It is a promising advanced control method that explicitly uses the system's model to predict its future changes. The basic idea of MPC is the

determination of the required control signals in advance [2].

Recent research works on grid connected CSI have focused on control strategies, new modified CSI topologies, improved modulation techniques, grid faults mitigation, resonance damping methods, and other. In [3] a CSI based static compensator (STATCOM) has been proposed using a new modelling method for the design of a state decoupled feed-back controller. Authors in [4] propose a decoupled active and reactive power control strategy for grid connected by acting on the modulation index and the angle of the pulse width modulator. In [5] a virtual flux based DPC for CSI is proposed for a grid connected wind application using a look-up table for the selection of the optimal current vector. In [6]–[8] the control of the powers is performed indirectly using two PI regulators to generate grid reference currents or modulation indexes of the PWM in the synchronously rotating frame (dq). In [9]–[11] New PWM techniques and switching patterns have been proposed to improve the power quality and reduce the switching frequency. Authors in [12]–[13] deal with grid faults and instabilities for grid connected CSIs. [14] proposes a power synchronization method without using PLL for grid tied CSIs.

This paper contributes by proposing an FS-MPDPC applied to grid connected CSI. In the literature, this method has been only applied for grid connected VSI, and power factor correctors based on PWM rectifiers. In this work the active and the reactive powers are predicted for the next sampling period, using a discrete prediction model which is constructed by predicting both the grid currents and voltages, then a cost function is introduced to find the best switching combination of the power switches to reach the desired references, also in this work a sequential minimal optimization (SMO) is designed in order to reduce the system's cost and complexity.

In addition to the introduction, this paper contains five other sections, in section II the topology and the model of the CSI are discussed, Section III presents the design of the proposed SMO. In section IV the proposed FS-MPDPC is presented, where the prediction model is mathematically derived using the system state space model, and the cost function is introduced for the selection of the command. Simulation results and discussions are presented in section V. Finally, Section VI concludes this work.

II. CSI TOPOLOGY AND MODEL

Figure 1 shows a three phase PWM CSI, which is usually composed of constant current source, a bridge of six unidirectional switches (reverse blocking IGBT, or IGBT in series with a diode), and a capacitive filter.

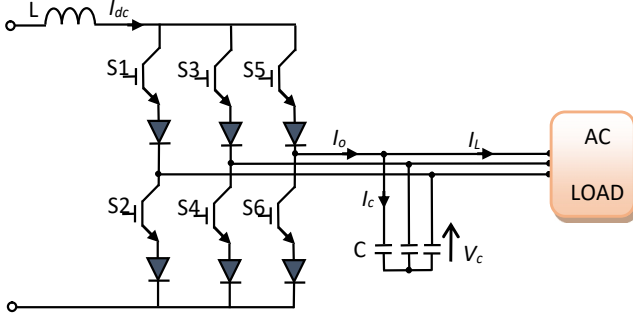


Fig. 1. Three phase CSI.

At any given time, the CSI must have at least one of the upper switches and one of the lower switches conducting simultaneously to ensure a current path for the DC source.

In addition, only one of the upper and lower devices can conduct at a time to ensure the output current waveform. These restrictions can be summarized as follows

$$S_1 + S_3 + S_5 = S_2 + S_4 + S_6 = 1. \quad (1)$$

The output currents can be defined according to the switching signals and the dc-current I_{dc} by:

$$I_{oa} = (S_1 - S_2)I_{dc}, \quad (2)$$

$$I_{ob} = (S_3 - S_4)I_{dc}, \quad (3)$$

$$I_{oc} = (S_5 - S_6)I_{dc}. \quad (4)$$

The coordinate transformation from $(a - b - c)$ to $(\alpha - \beta)$ is obtained using Clark's transformation matrix given by

$$\begin{bmatrix} u_{o\alpha} \\ u_{o\beta} \end{bmatrix} = \frac{2}{3} \begin{bmatrix} 1 & -\frac{1}{2} & -\frac{1}{2} \\ 0 & \frac{\sqrt{3}}{2} & -\frac{\sqrt{3}}{2} \end{bmatrix} \begin{bmatrix} u_{oa} \\ u_{ob} \\ u_{oc} \end{bmatrix}. \quad (5)$$

And the space vector is obtained as

$$u(t) = u_{o\alpha}(t) + ju_{o\beta}(t) = u_m(t)e^{j\omega t}, \quad (6)$$

where u is generic variable, and u_m is its magnitude.

The valid switching states with corresponding phase current, and current vectors are presented in Table. I

Using the space vector representation, the grid connected CSI can be modelled by these equations:

$$\dot{\vec{i}}_o = C \frac{d\vec{V}_c}{dt} + \vec{i}_g, \quad (7)$$

$$\vec{V}_c = R_f \vec{i}_g + L_f \frac{d\vec{i}_g}{dt} + \vec{v}_g, \quad (8)$$

where i_o is the CSI output current vector (Fig. 3), i_g is the grid current vector, V_c is capacitor filter voltage vector, R_f

and L_f are the resistance and the inductance of the inductor, And C is the capacitance of the capacitor filter.

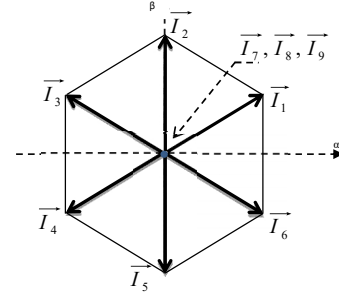


Fig. 1. CSI output current vectors.

TABLE I. CSI POSSIBLE STATES AND CURRENT VECTORS.

Switches						Phase current			Current vector
1	2	3	4	5	6	ILa	ILb	ILc	
1	0	0	0	0	1	I_{dc}	0	$-I_{dc}$	$\vec{i}_1 = 2I_{dc}e^{(j\pi/6)} / 3^{1/2}$
0	0	1	0	0	1	0	I_{dc}	$-I_{dc}$	$\vec{i}_2 = 2I_{dc}e^{(j\pi/2)} / 3^{1/2}$
0	1	1	0	0	0	$-I_{dc}$	I_{dc}	0	$\vec{i}_3 = 2I_{dc}e^{(j5\pi/6)} / 3^{1/2}$
0	1	0	0	1	0	$-I_{dc}$	0	I_{dc}	$\vec{i}_4 = 2I_{dc}e^{(j7\pi/6)} / 3^{1/2}$
0	0	0	1	1	0	0	$-I_{dc}$	I_{dc}	$\vec{i}_5 = 2I_{dc}e^{(j3\pi/2)} / 3^{1/2}$
1	0	0	1	0	0	I_{dc}	$-I_{dc}$	0	$\vec{i}_6 = 2I_{dc}e^{(j11\pi/6)} / 3^{1/2}$
1	1	0	0	0	0	0	0	0	$\vec{i}_7 = 0$
0	0	1	1	0	0	0	0	0	$\vec{i}_8 = 0$
0	0	0	0	1	1	0	0	0	$\vec{i}_9 = 0$

III. SEQUENTIAL MINIMAL OPTIMIZATION (SMO)

State observers are used for both technical and economic reasons, by reducing the system's cost and complexity, and avoiding the noise of the sensors.

Unlike other state observers, in SMOs, instead of feeding back the output error between the observer and the system linearly, the output error is fed back via a discontinuous switched signal.

From (7) and (8) the mathematical model of the system can be defined as:

$$\frac{d}{dt} i_g = \frac{V_c}{L_f} - \frac{R_f}{L_f} i_g - \frac{V_g}{L_f}, \quad (9)$$

$$\frac{d}{dt} V_c = \frac{1}{C} i_o - \frac{1}{C} i_g. \quad (10)$$

By means of the above mentioned system model, and using the sliding mode theory, the proposed SMO can be modelled as follows:

$$\frac{d}{dt} \hat{i}_g = \frac{\hat{V}_c}{L_f} - \frac{R_f}{L_f} \hat{i}_g - \frac{V_g}{L_f} + k \cdot \text{Sgn}(i_g - \hat{i}_g), \quad (11)$$

$$\frac{d}{dt} \hat{V}_c = \frac{1}{C} i_o - \frac{1}{C} \hat{i}_g + k' \cdot \text{Sgn}(i_g - \hat{i}_g), \quad (12)$$

where $(\hat{\quad})$ denotes an estimated value.

The sliding surface (S) is constructed using the error between the measured and the estimated grid current ($i_g - \hat{i}_g$).

In this SMO a saturation function is used instead of the sign function to reduce the undesirable problem of chattering, the applied saturation function is defined below

$$\text{Sat}(S) = \begin{cases} 1, & \text{if } S > \Delta, \\ S/\Delta, & \text{if } -\Delta < S < \Delta, \\ -1, & \text{if } S < -\Delta, \end{cases} \quad (13)$$

where Δ is a tuning parameter.

IV. P-DPC FOR GRID CONNECTED CSI

Predictive control methods present many advantages that make them suitable for the control of power converters. The concepts are intuitive and easy to understand; it can also be applied to a variety of systems; constraints and nonlinearities can be easily included, and the resulting controller is easy to implement. Generally, the quality of the controller depends on the quality of the model [2].

A. Prediction Model

In this structure, the grid currents and voltages are measured, and the capacitor filter voltages are estimated using the SMO. These measures are necessary to predict the behaviour of the controlled variables, which are the active and the reactive power.

The instantaneous active and reactive power of the grid are expressed in terms of the grid currents and voltages, in the stationary frame by:

$$P = i_{g\alpha} \cdot V_{g\alpha} + i_{g\beta} \cdot V_{g\beta}, \quad (14)$$

$$Q = i_{g\alpha} \cdot V_{g\beta} - i_{g\beta} \cdot V_{g\alpha}. \quad (15)$$

Thus, the predicted powers can be written as follows:

$$P(k+1) = i_{g\alpha}(k+1) \cdot V_{g\alpha}(k+1) + i_{g\beta}(k+1) \cdot V_{g\beta}(k+1), \quad (16)$$

$$Q(k+1) = i_{g\alpha}(k+1) \cdot V_{g\beta}(k+1) - i_{g\beta}(k+1) \cdot V_{g\alpha}(k+1). \quad (17)$$

For the prediction model an approximation in the discrete-time is considered, such as for a generic variable x [2]

$$\frac{dx}{dt} \approx \frac{x(k+1) - x(k)}{T_s}. \quad (18)$$

By application of the approximation in (18) into equation (7) and (8), and after a mathematical analysis the nine possible output current predictions can be obtained from the above mentioned equations, as follows

$$i_g[k+1] = \frac{T_s}{R_f T_s + L_f} \times \left(\frac{T_s}{C} i_o[k] + V_c[k] - V_g[k] + \frac{L_f C - T_s^2}{C T_s} i_g[k] \right). \quad (19)$$

The grid voltage predictions are given by

$$V_g(k+1) = V_g e^{j\Delta\theta}, \quad (20)$$

where $\Delta\theta = \omega \cdot T_s$.

B. Cost Function

The nine predicted active and reactive power are compared with their references using a cost function g given by

$$g_i = \left\| P^* - P[k+1] \right\| + \left\| Q^* - Q[k+1] \right\|, \quad (21)$$

where i denotes the index of the inverter current vector used in the predictions.

Finally, the current vector that minimizes this cost function is chosen and applied to the inverter in the next sampling period. The control algorithm of FS-MPDPC is shown in Fig. 3.

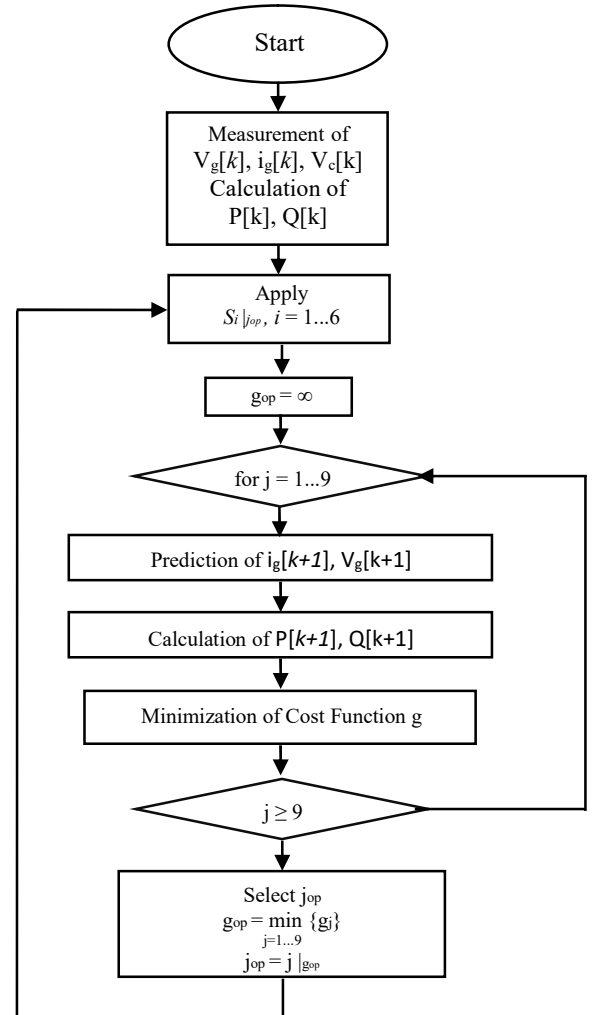


Fig. 3. FS-MPDPC control algorithm.

V. SIMULATION RESULTS AND DISCUSSION

In order to evaluate the performance of the proposed FS-MPDPC with the SMO, the set-up of Fig. 4 has been simulated in MATLAB/Simulink® environment, using the parameter values listed in Table II.

TABLE II. ELECTRICAL PARAMETERS OF THE POWER CIRCUIT.

Quantity	Value
Dc current I_{dc}	20 (A)
Output capacitor filter C	$150 \cdot 10^{-6}$ (F)
Grid Voltage (RMS) V_g	50 (V)
filter resistance R_f	0.1 (Ω)
filter inductance L_f	0.01 (H)
Sample time T_s	$25 \cdot 10^{-6}$ (s)

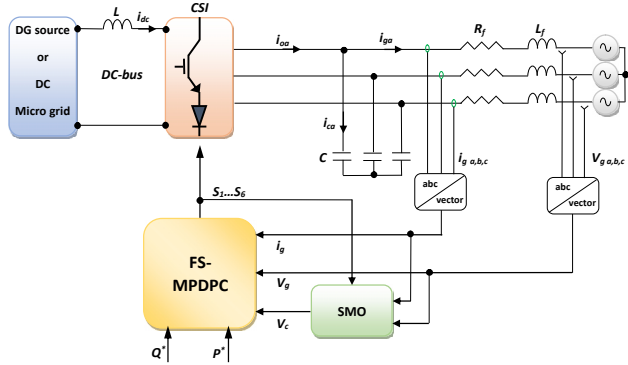


Fig. 4. Proposed FS-PDPC control scheme.

Different scenarios for active and reactive references has been simulated, such as from 0 to 0.2 s and from 0.7 s to 1 s only active power is injected to the grid, from 0.3 s to 0.6 s only reactive power is injected to the grid, and both powers are injected to the grid in the rest of simulation time.

Figure 5(a) and Fig. 5(b) show the transient response for active and reactive powers respectively. It can be seen that they follow their references rapidly, with low ripple, and without overshoot during sudden reference changes.

Figure 5(c) shows the three phase currents injected to the grid. It is remarkable that the currents are practically sinusoidal with low harmonic distortion. This can be confirmed in Fig. 5(d) which shows the spectrum of the grid current, where the Total harmonic distortion (THD) was about 2.32 % which agrees with IEEE standards.

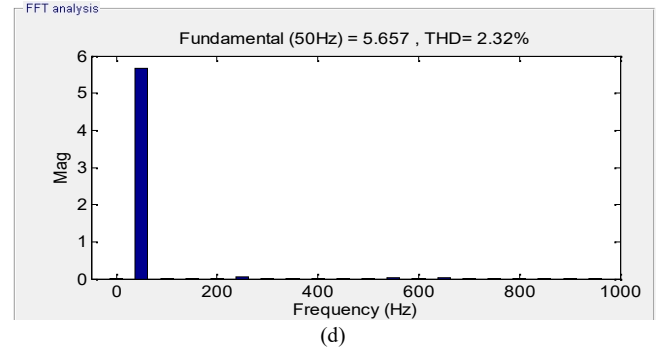
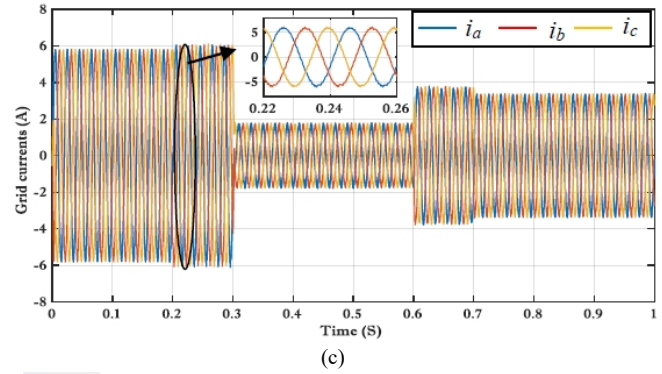
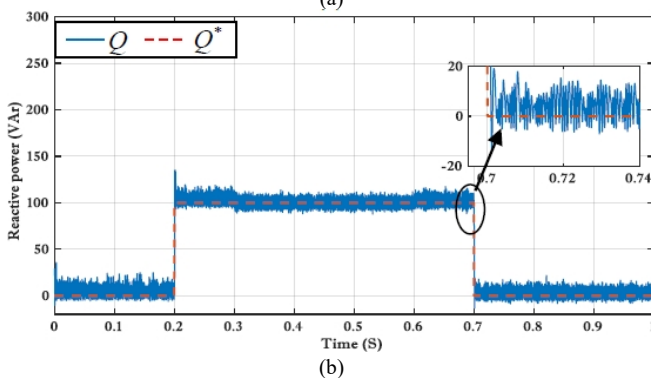
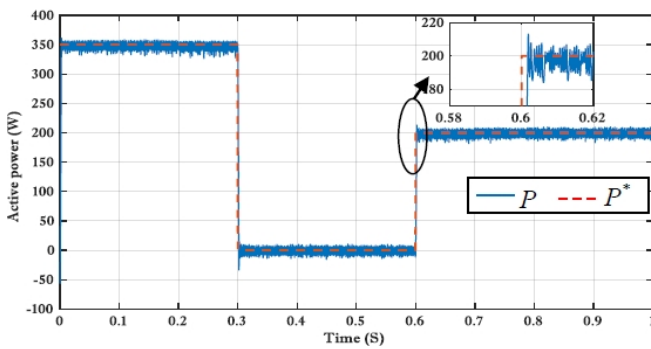
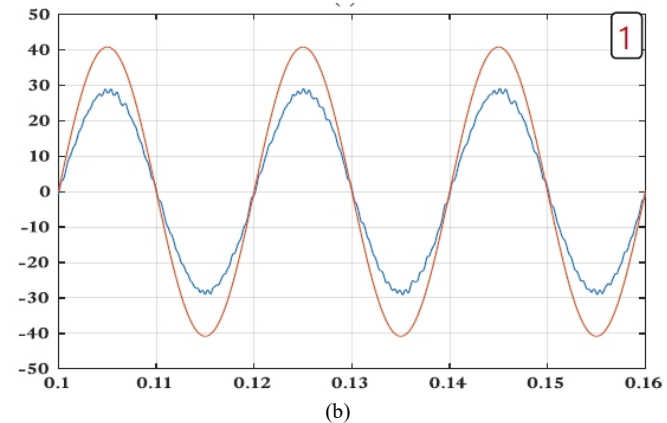
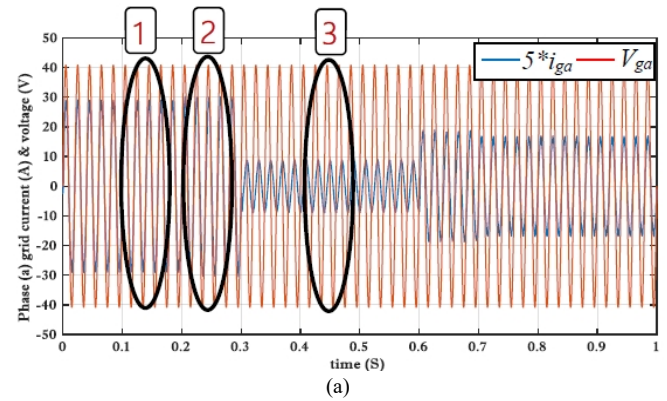


Fig. 5. Transient response of the system for: (a) – active power, (b) – reactive power, (c) – grid currents, (d) – spectrum of the grid currents.

Figure 6(a) shows the phase (a) current and voltage, and Fig. 6(a)–Fig. 6(c) show three different zooms during each of the above mentioned power injection scenarios. The first zoom (Fig. 5(a)) was performed during active power injection. It is obvious that the current and the voltage are in phase. In Fig. 5(b) the current and the voltage are not in phase, because of the reactive power injection. In the third zoom the phase between the current and the voltage is $\pi/2$ which means that only reactive power is injected into the grid.



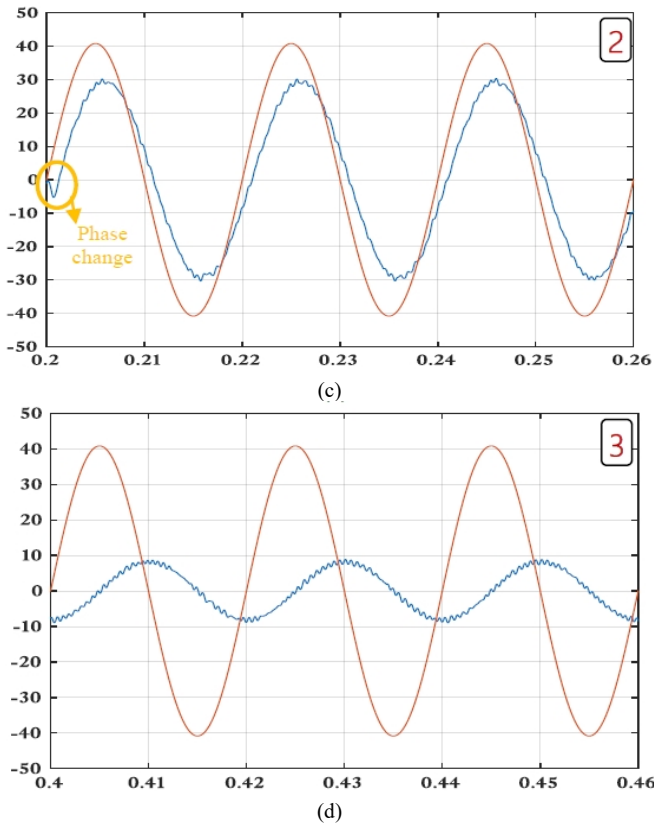


Fig. 6. Phase (A) Grid current and voltage with different zooms: (a) – waveforms of voltages and currents, (b) – zoom case 1, (c) – zoom case 2, (d) – zoom case (3).

Figure 7 shows the effectiveness of the SMO which has succeeded in providing nearly the same measured filter voltages.

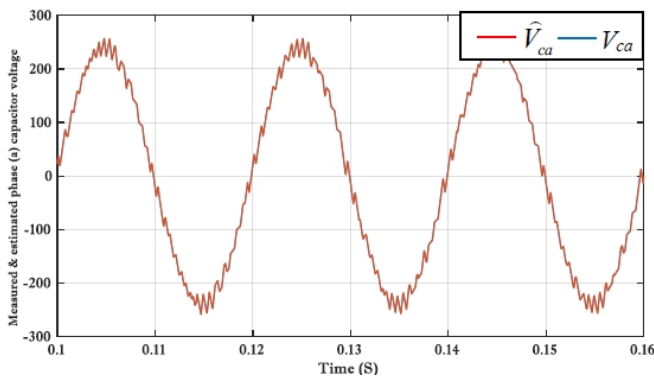


Fig. 7. Waveforms of measured and observed phase (A) capacitor filter voltage.

VI. CONCLUSIONS

A new control strategy for grid connected CSI has been proposed based on DPC and MPC called FS-MPDPC. This strategy offers simplicity, decoupled control for active and reactive powers, fast response, and good output currents with low harmonic distortion. Furthermore, as compared with other control techniques in the same field the suggested technique is PLL-less.

The FS-MPDPC is based on the prediction of the future changes in active and reactive powers using a discrete time prediction model, these predictions are then evaluated by the means of a cost function which generates the control signals.

The obtained simulation results demonstrate the good performance of the proposed method. Where the grid's active and reactive powers are controlled separately with fast response, low ripple, small overshoot, and good current waveforms. It was presented also the performance of the SMO which has succeeded in estimating the filter voltages with practically negligible error.

REFERENCES

- [1] H. Abu-Rub, M. Malinowski, K. Al-Haddad, *Power electronics for renewable energy systems, transportation and industrial applications*. John Wiley & Sons Ltd.: New Jersey, USA, 2014. [Online]. Available: <https://doi.org/10.1002/9781118755525>
- [2] J. Rodriguez, P. Cortes, *Predictive control of power converters and electrical drives*. New Jersey: John Wiley & Sons Ltd., USA, 2012. [Online]. Available: <https://doi.org/10.1002/9781119941446>
- [3] S. Jayalath, M. Hanif, "CL-Filter design for grid-connected CSI", *IEEE 13th Brazilian Power Electronics Conf. and 1st Southern Power Electronics Conf. (COBEP/SPEC)*, 2015, pp. 1–6. [Online]. Available: <https://doi.org/10.1109/COBEP.2015.7420090>
- [4] M. Saghaleini, B. Mirafzal, "Power Control in Three-Phase Grid-Connected Current-Source Boost Inverter", *Energy Conversion Congress and Exposition (ECCE)*, 2011, pp. 776–783. [Online]. Available: <http://dx.doi.org/10.1109/ECCE.2011.6063849>
- [5] A. Nikolic, B. Jcftenic, "Direct torque control and virtual-flux based direct power control of current source converter in wind turbine application", in *Proc. 14th European Conf. Power Electronics and Applications*, Birmingham, UK, 2011, pp. 1–10.
- [6] P. P. Dash, M. Kazerani, "Dynamic modeling and performance analysis of a grid-connected current-source inverter-based photovoltaic system", *IEEE Trans. Sustainable Energy*, vol. 2, no. 4, pp. 443–450, 2011. [Online]. Available: <http://dx.doi.org/10.1109/TSTE.2011.2149551>
- [7] S. Anand, S. K. Gundlapalli, B. G. Fernandes, "Transformer-less grid feeding current source inverter for solar photovoltaic system", *IEEE Trans. Ind. Electron*, vol. 61, no. 10, pp. 5334–5344, 2014. [Online]. Available: <http://dx.doi.org/10.1109/TIE.2014.2300038>
- [8] T. Geury, S. Pinto, J. Gyselinck, "Current source inverter-based photovoltaic system with enhanced active filtering functionalities", *IEEE Trans. Power. Electron*, vol. 8, no. 12, pp. 2483–2491, 2015. [Online]. Available: <http://dx.doi.org/10.1049/iet-pel.2014.0814>
- [9] A. Morsy, S. Ahmed, A. M. Massoud, "Harmonic rejection in current source inverter-based distributed generation with grid voltage distortion using multi-synchronous reference frame", *IET Power. Electron*, vol. 7, no. 6, pp. 1323–1330, 2014. [Online]. Available: <http://dx.doi.org/10.1049/iet-pel.2013.0186>
- [10] S. A. Azmi, G. P. Adam, B. Williams, "New direct regular-sampled pulse-width modulation applicable for grid and islanding operation of current source inverters", *IET Power. Electron*, vol. 7, no. 1, pp. 220–236, 2014. [Online]. Available: <http://dx.doi.org/10.1049/iet-pel.2013.0235>
- [11] K. Gnanasambandam, A. Edpuganti, A. K. Rathore, D. Srinivasan, C. Cecati, C. Buccella, "Optimal low switching frequency pulse width modulation of current-fed three-level converter for solar power integration", *IEEE Trans. Ind. Electron*, vol. 63, no. 11, pp. 6877–6886, 2016. [Online]. Available: <http://dx.doi.org/10.1109/TIE.2016.2586019>
- [12] V. Vikhande, K. V. Kanakesh, B. G. Fernandes, "Control of three-phase bidirectional current source converter to inject balanced three-phase currents under unbalanced grid voltage condition", *IEEE Trans. Power. Electron*, vol. 31, pp. 6719–6737, 2016. [Online]. Available: <http://dx.doi.org/10.1109/TPEL.2015.2503352>
- [13] A. A. A. Radwan, Y. A. I. Mohamed, "Analysis and active suppression of AC- and DC-side instabilities in grid-connected current-source converter-based photovoltaic system", *IEEE Trans. Sustainable Energy*, vol. 4, no. 3, pp. 630–642, 2013. [Online]. Available: <http://dx.doi.org/10.1109/TSTE.2012.2230653>
- [14] A. A. A. Radwan, Y. A. I. Mohamed, "Power synchronization control for grid-connected current-source inverter-based photovoltaic systems", *IEEE Trans. Energy. Conversion*, vol. 31, pp. 1023–1036, 2016. [Online]. Available: <http://dx.doi.org/10.1109/TEC.2016.2533630>